Pergamon

Cement and Concrete Research 33 (2003) 525–538

CEMENT AND CONCRETE RESEARCH

An acousto-ultrasonic approach for the determination of water-to-cement ratio in concrete

T.P. Philippidis[a,*], D.G. Aggelis[b]

[a]Department of Mechanical Engineering and Aeronautics, University of Patras, P.O. Box 1401, Patras 26500, Greece
[b]Institute of Chemical Engineering and High Temperature Chemical Processes (ICEHT-FORTH), Patras, Greece

Received 6 February 2002; accepted 16 September 2002

Abstract

A novel nondestructive procedure for the evaluation of water-to-cement (w/c) ratio in concrete is presented. The experimental setup is based on the method of acousto-ultrasonics; data analysis, however, and recognition of concrete composition from the waveform transmitted through specimen thickness, are achieved by simple time and frequency domain schemes used in this work. Experiments were performed in a number of concrete specimens made at various w/c ratios and at a number of ages starting from 2 up to 90 days. Recognition results were satisfactory and the algorithm introduced was successful in identifying the correct w/c ratio in more than 90% of the test cases. The use of existing spectral analysis techniques such as the coherence function has also proved to be more efficient and fits the purpose. The possibility of water content determination in fresh paste is also discussed along with preliminary evidence from initial tests.

Keywords: Nondestructive evaluation; Concrete; Cement paste; Characterization; Water to cement ratio

1. Introduction

The nondestructive testing (NDT) of concrete, especially related to strength determination, is a scientific area concentrating great interest and research work. One of the factors affecting crucially concrete's performance is the water content (water-to-cement ratio, w/c) [1]. If this ratio is held below a certain value at mixing, the durability and strength of concrete are assumed to be of acceptable standards at later ages. Generally, the strength of concrete is characterized by the result of compressive tests at 28 days after placing. However, quality evaluation at earlier ages, even fresh concrete, is highly desirable.

Several nondestructive techniques based on the stress wave analysis have been developed for assessing quality of concrete. Wave propagation is strongly affected by the elastic properties and density of constituent materials. Thus, it is assumed to be indicative of structural integrity parameters. So far, elastic wave velocity has extensively been used to estimate concrete strength (e.g. Refs. [2,3]). Models for 28 and 90 days compressive strength prediction, based on 1 and 2 days velocity measurements, have been proposed [3]. The dependence of w/c ratio on ultrasonic pulse velocity for both concrete and mortar has also been studied [2,4], although the number of specimens tested in these works is considered inadequate for accurate determination of w/c ratio. For cases where thickness ultrasonic examination is impossible, surface wave velocity was shown to yield accurate predictions of strength [5]. Effort has also been given in the testing of fresh concrete [6] and mortar either with through-transmission [7–11] or reflection techniques [12–15]. Research in this field, however, is concentrated in the monitoring of the hardening process and the estimation of the set time that is of particular interest for certain applications [16–18] instead of reliable water content estimation. Study of the water content influence on the propagating wave is just qualitative in the above works and no sufficient data for the reliable estimation of w/c ratio of the freshly mixed material are provided. Additionally, measurements are not conducted for at least 15 min after mixing or even more, with the exception of Ref. [19], while the difference in w/c ratio seems to have a clearer influence on the wave velocity after the first hours.

* Corresponding author. Tel./fax: +30-610-997235.
E-mail address: philippidis@mech.upatras.gr (T.P. Philippidis).

0008-8846/02/$ – see front matter © 2002 Elsevier Science Ltd. All rights reserved.
PII: S0008-8846(02)00999-7

A comprehensive literature survey on the usual nondestructive methods used for concrete testing, concerning either ultrasound or other techniques, can be found in Refs. [20,21].

Herein, a method of reliable estimation of w/c ratio of concrete is presented. The method has been applied to mortar and concrete specimens of various ages, yielding reliable estimation of the w/c ratio from the second day. It is based on simple time and frequency domain analysis schemes of signals acquired by means of an acousto-ultrasonic (AU) setup.

This work was undertaken in the framework of a National project aiming at the development of a methodology for nondestructive quality of concrete evaluation from the first days or even when still in fresh state. The project involved AU examination of several compositions of mortar and concrete, along with destructive tests for compressive strength and parameters of microstructure determination, in order to correlate wave propagation characteristics with properties of concrete and especially water content. Mortar testing preceded that of concrete and the methodology presented here was first applied for mortar evaluation. Although classification results from testing of mortar specimens were very good, the population of the sample is considered adequate just for preliminary conclusions to be drawn and thus only results from concrete tests are presented herein as they are based on a statistically more significant population.

Simultaneously, work was conducted towards characterization of fresh paste, although the establishment of an AU setup, along with a wave analysis methodology, proved to be much more complicated and results as to w/c ratio recognition less successful.

2. The AU method

The classic AU arrangement consists of two piezoelectric sensors attached to the object being examined. One of the transducers is excited using an ultrasonic pulser and the other is used as a typical acoustic emission (AE) sensor. Therefore, the method detects characteristics of the stress wave propagation occurring within the object at a location some distance from the position of the excitation. It was introduced for estimation of mechanical properties in composite structures [22] but has been proven successful also in inspection of adhesive bond integrity [23], determination of plate wave velocities [24], porosity evaluation of polymer structures [25], inspection of biodeterioration in utility poles [26]. Generally, the method is used for monitoring of distributed properties, e.g. damage, porosity, instead of searching for specific flaws [27].

The original AU procedure used a single descriptor of the waveform, called the stress wave factor (SWF) or counts, which is the number of oscillations of the signal above a selected voltage threshold. Some other important features are amplitude (absolute voltage of the highest waveform peak), energy (area under the rectified waveform), duration (time elapsed between the first and the last threshold crossing), etc. These parameters are measured in real time using dedicated circuitry. In the work presented in this paper, due to the significant variance exhibited by these time domain characteristics for various w/c classes, a more elaborate analysis of the waveforms was employed, resulting in an almost excellent classification as to the water content of concrete.

3. Hardened concrete

3.1. Experimental procedure

3.1.1. Test methodology and equipment

The experimental setup used in this work is shown in Fig. 1. The pulse generator gives rise to an electrical impulse, of duration practically about 10 μs, which is transferred as a stress wave into the specimen by means of a piezoelectric transducer of low resonant frequency, attached to the center of one surface. The stress wave propagates through the material and it excites another sensor of the same type, which is attached on the opposite surface. This signal is then preamplified, digitized and stored as a waveform (Fig. 2).

A metallic jig is used in order to assure steady pressure on the sensors, which are directly attached to the surface of the specimen (see Fig. 3), while a layer of grease is applied in the sensor and concrete interface to assure acoustical coupling. The equipment used consists of two piezoelectric transducers R6 of Physical Acoustics Corporation (PAC), resonant nominally in the range 20–120 kHz, pulse gen-

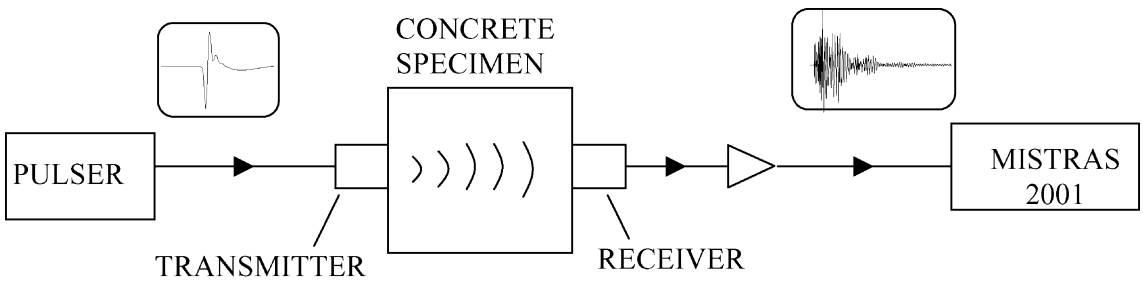

Fig. 1. Schematic representation of the AU experimental setup.

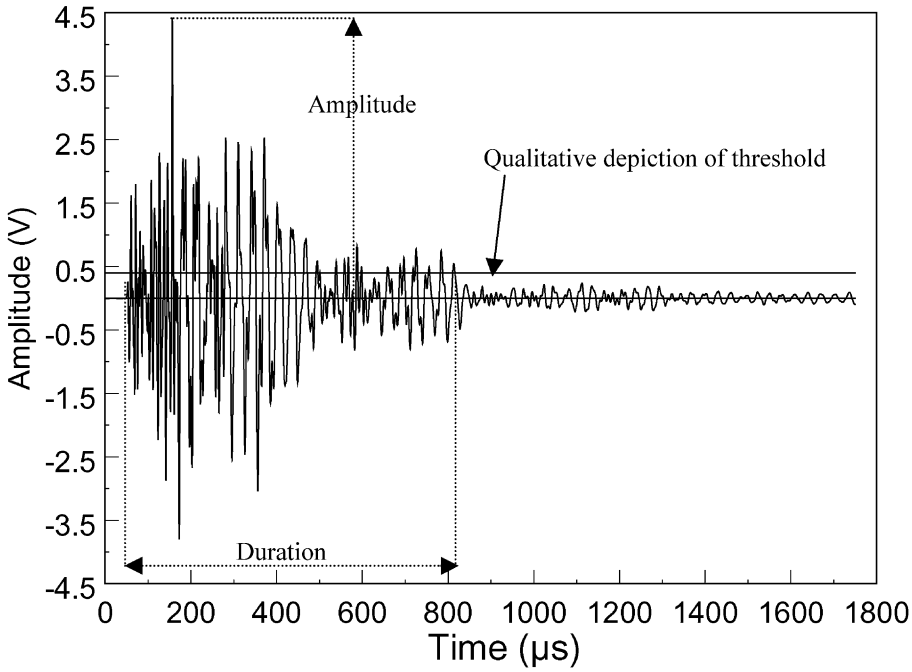

Fig. 2. A typical waveform with its basic descriptors.

erator PAC C101-HV, PAC 1220A pre-amps and a MISTRAS 4 channel data acquisition system. The 16-bit A/D board ensures accurate depiction of the waveform through the resolution of 0.305 mV. Waveforms were captured at a sampling rate of 2 MHz, which is considered adequate since the frequency range of high sensitivity of R6 sensors is below 200 kHz. Details on the experimental setup are also given in Ref. [28].

3.1.2. Materials and specimen geometry

High-strength Portland cement was used while the aggregates were of limestone origin and their maximum size was 37.5 mm. The preparation procedure followed the New Greek standard of concrete technology 97 (ΣΚ 303), which is in accordance with ASTM C192, and took place at the Greek Center for Cement Research (EKET); 150 mm cubic specimens were used, the aggregate to cement ratio being

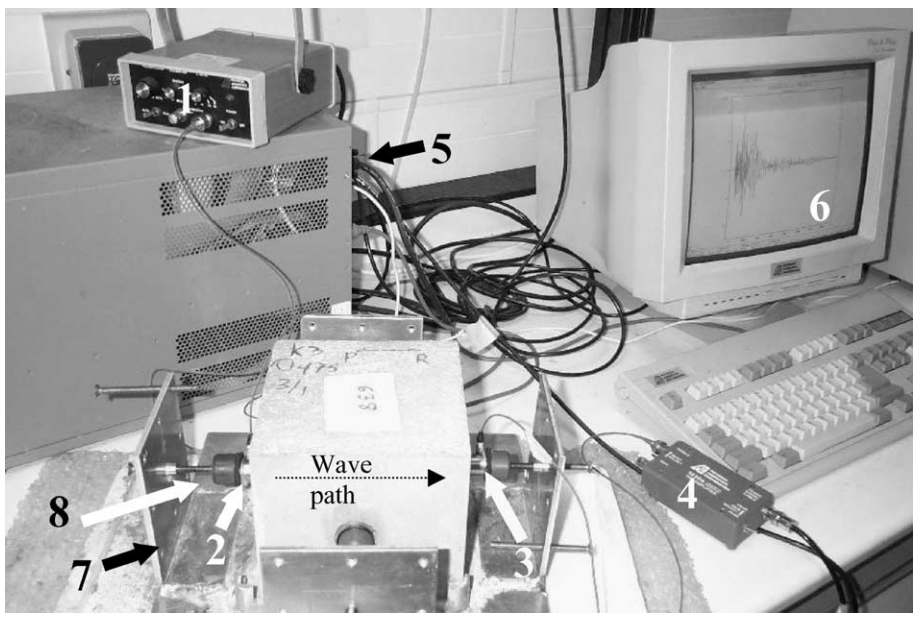

Fig. 3. The experimental arrangement. (1) Pulse generator, (2) transducer, (3) receiver, (4) preamplifier, (5) DAQ system, (6) acquired waveform, (7) supporting jig, (8) bolt and rubber pad.

a/c = 3, while four different w/c ratios were tested, from 0.375 to 0.45 at a step of 0.025.

Specimen preparation and tests were divided in two different experimental phases, the first held in year 2000 and the second one in 2001. In total, 14 specimens were ultrasonically tested from w/c = 0.375 class, 12 from classes 0.40, 0.425, and 16 specimens from class 0.45. The measurements were repeated seven times throughout the first 90 days of concrete's life, namely, 2, 4, 7, 14, 28, 60 and 90 days. Compressive tests took place at the ages of 2, 7, 28 and 90 days on cubes of the same mixture as the ones used for the AU tests [28].

3.2. Results and discussion

3.2.1. Correlation of AU descriptors with the hydration process and strength

Apart from the characteristic descriptors of the waveform, longitudinal wave velocity was calculated as well by measuring the time difference between the first threshold crossing of the emitted and the received signals. Tests conducted at different ages revealed considerable changes in wave propagation characteristics. Higher velocities were measured at later ages, as expected, accompanied by higher waveform amplitude. In Fig. 4, waveforms of the same specimen, with w/c = 0.4, are presented for the ages of 2 and 90 days. It is obvious that the hardening process due to the hydration reaction taking place in concrete results in an increase of the elastic energy transmitted, through the stiffening of the mortar matrix.

We should mention that the long signal duration is formed by a combination of potential reflection arrivals and the so-called ringing behavior of these sensitive AE transducers, implying that given an initial excitation, the sensor response exhibits a series of reverberations according to its frequency sensitivity. Although this behavior somehow "masks" the pure wave propagation characteristics and makes the discrimination of reflection arrivals troublesome, using the same type of sensors throughout the whole experimental series assures that any changes in the obtained signal is attributed to the different material and allows for valid comparisons between specimens of different composition and age to be made.

Water content also has a significant impact on the acquired signals as seen in Fig. 5(a) and (b), where waveforms of specimens of different composition, w/c = 0.375 (a) and 0.45 (b), are presented for the age of 2 days. It is obvious that the higher amplitude waveform belongs to w/c = 0.375 specimen. The higher peak amplitude for low water content is only a general trend however, and in some cases, waveforms originating from higher w/c specimens exhibit peak amplitude of the same or higher voltage than waveforms of low w/c (see Fig. 5(c) and (d)). The influence of water content on wave propagation will be treated thoroughly later in this paper.

Further processing of waveforms reveals an increasing trend of time domain characteristics with age as observed in Figs. 6 and 7, where the waveform peak amplitude and dimensionless signal energy for various ages are depicted for all different compositions of specimens. The lines are drawn

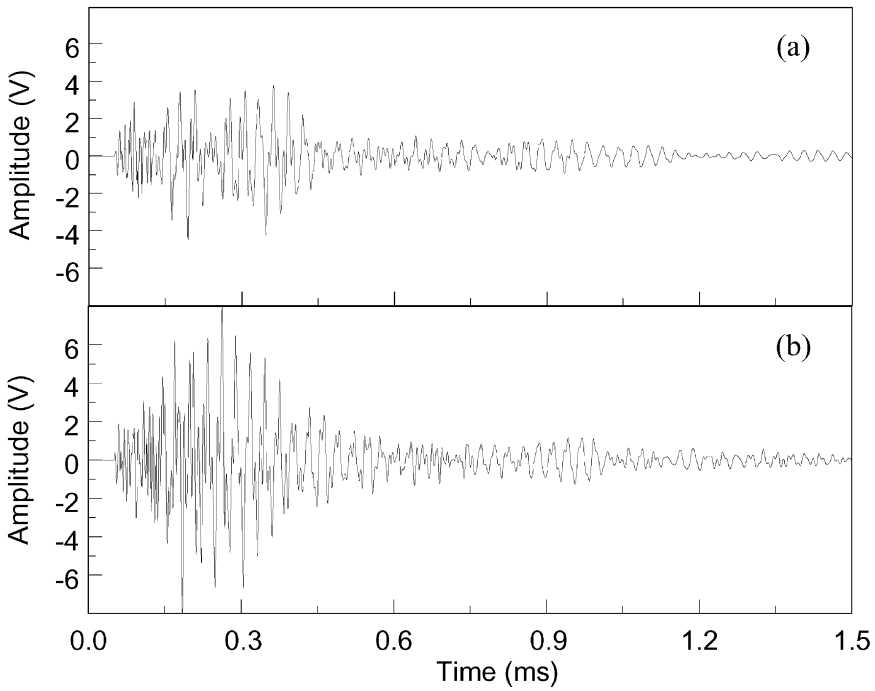

Fig. 4. Effect of age on waveform characteristics, w/c = 0.40. (a) 2 days, (b) 90 days.

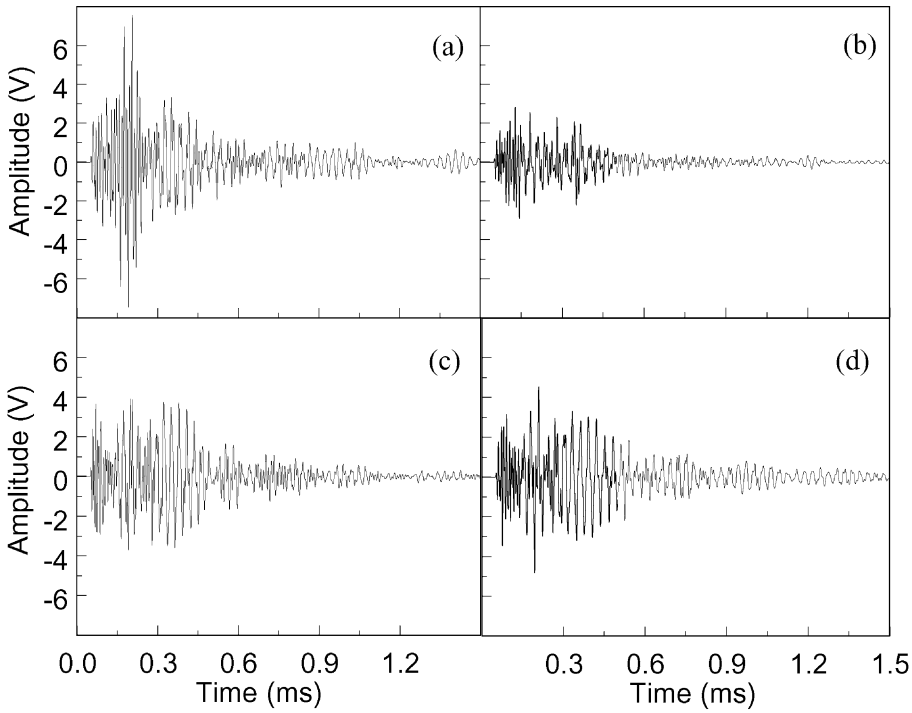

Fig. 5. Effect of w/c ratio on generated waveforms. (a) w/c = 0.375, (b) w/c = 0.45, (c) w/c = 0.375, (d) w/c = 0.40 for the age of 2 days.

using the average values of the population of each composition. The parameter energy is presented in a dimensionless form (energy counts) being proportional to the measured area of the rectified signal envelope. Henceforth, it will be denoted as energy.

The changes are substantial throughout the first week, but tend to disappear at ages older than 28 days. This trend approaches the typical well-known logarithmic increment that describes the hydration process [1], implying that changes in wave propagation characteristics are due to this process. This is confirmed as the characteristics of the waveforms exhibit linear correlation with strength and have been used successfully for strength estimation at any age [29]. An example is given in Fig. 8 where a comparison of compressive strength and waveform energy for two different composition classes yields strong linear correlation. Although the trend is clear, the lack of an adequate number of points does not allow the establishment of a robust prediction model.

3.2.2. Water content influence on wave propagation

As indicated by the different waveforms of Fig. 5 and also known previously (e.g., Ref. [2]), w/c ratio has a net influence on the propagating wave. It was also clear in Figs. 6

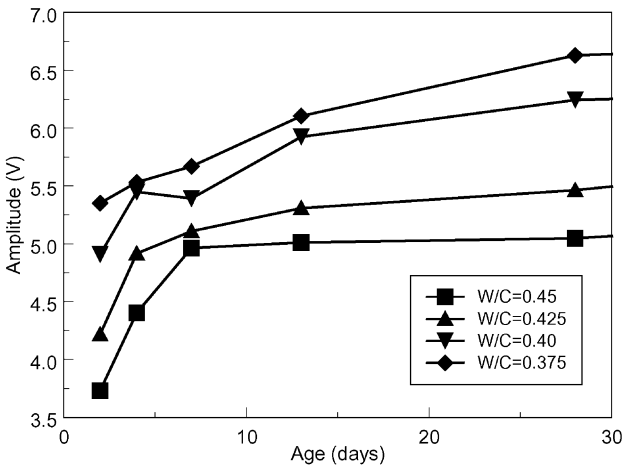

Fig. 6. Waveform peak amplitude versus age.

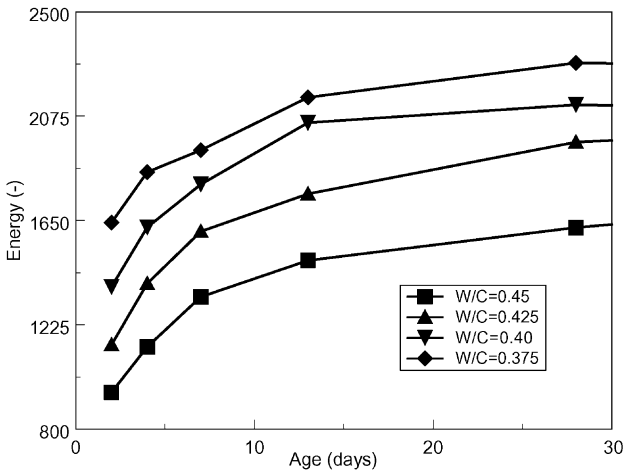

Fig. 7. Energy versus age.

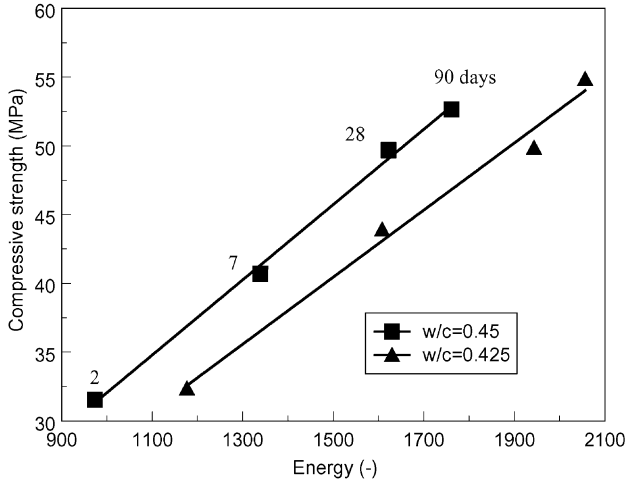

Fig. 8. Correlation of compressive strength and signal energy of w/c = 0.45 and w/c = 0.425 specimens.

and 7 that lower w/c ratios result in higher average values of wave descriptors, which was expected as a change in w/c affects the modulus of elasticity and porosity of the hardened cement paste. Nevertheless, the scatter is quite significant as seen in Fig. 9 where the variation of counts versus w/c for the age of 2 days and that of energy versus w/c for the age of 7 days are presented. The symbols on the above diagrams represent averages, while error bars stand for maximum and minimum measured values. Additionally, velocity measurements, although following the known decreasing behavior with the increase of water content [2,4], exhibited significant variance, as seen in Fig. 10(a), which makes velocity a weak wave characteristic to use for concrete composition identification. It should be mentioned, however, that velocity proved a highly powerful descriptor for w/c ratio determination in mortar, as it exhibited less variance and the difference in velocity values between specimens of different w/c ratio was clear, as indicated in Fig. 10(b).

From the above, it is obvious that the overlap exhibited by the time domain characteristics does not allow reliable estimation of w/c ratio of a concrete specimen based on a single feature of the waveform. In that respect, the classical AU approach is of limited value and more sophisticated analysis should be sought.

3.3. Classification approach

For the problem at hand, i.e. discrimination between the members of different classes, representing concrete of varying w/c ratios, the use of a single standard AE waveform descriptor was not proven powerful as in other cases [22]. However, since each concrete specimen as member of a class can be represented by a vector (pattern) whose n components are its waveform features, more sophisticated, multivariate statistical analysis approaches can be used to correctly recognize each pattern. In that respect, one needs to use as many components of each pattern as to assure the conditions for successful mathematical pattern recognition in the n-dimensional space. This implies the definition of waveform descriptors with high discriminative power not only from the time domain but also from alternatives offered by signal transforms in various domains such as frequency, cross-correlation, etc. In processing that way the waveforms of the entire database, simple, albeit efficient, procedures were adopted for classification of the signals, exploiting the similarities between signals of the same origin which lie either in the time or in the frequency domain.

3.3.1. Introduction of the cross-correlation scheme

Consider the waveforms, $X_1(t)$ and $X_2(t)$, of two different specimens that belong to the same w/c class recorded at the same age shown in Fig. 11. The similarity of these waveforms is apparent. Their product has the shape of the curve shown in Fig. 12. It is reminded here that the average value of this function is the value of the cross-correlation function for time lag equals zero, $R_{xy}(0)$. An amount of positive area under the product curve, and also a negative one, is observed. It was revealed that, the ratio of positive to negative area is high generally when the waveforms belong to the same composition. In the example of Fig. 12, it is equal to 9.19. Instead, the product of waveforms that belong to different w/c class exhibit low ratio of positive to negative area, as seen in Fig. 13 where the product of a 2-day w/c = 0.45 waveform and a 0.40 is presented and the ratio is calculated to be equal to 0.69. This may be attributed to the "synchronization" that exists between waveforms of the same mixture, originating from the wave propagation features typical of each class.

Generally, in waveforms of specimens of the same w/c ratio, positive and negative peaks rise and fall, respectively, at the same time, resulting in positive values when multiplied. This fact could suggest a difference also in the Fourier transforms of the signals. However, difference was

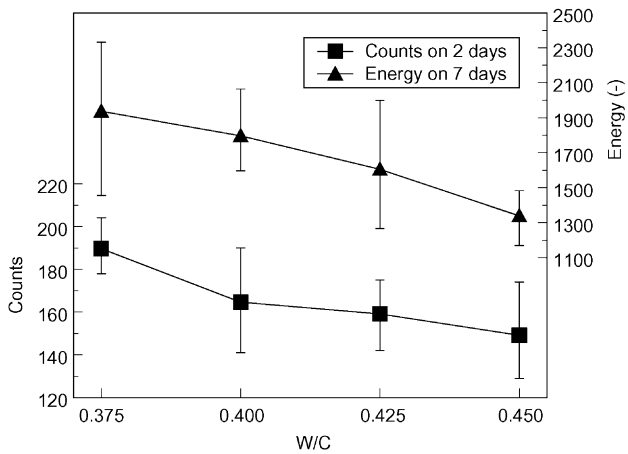

Fig. 9. Waveform counts for the age of 2 days and waveform energy of 7 days versus w/c ratio.

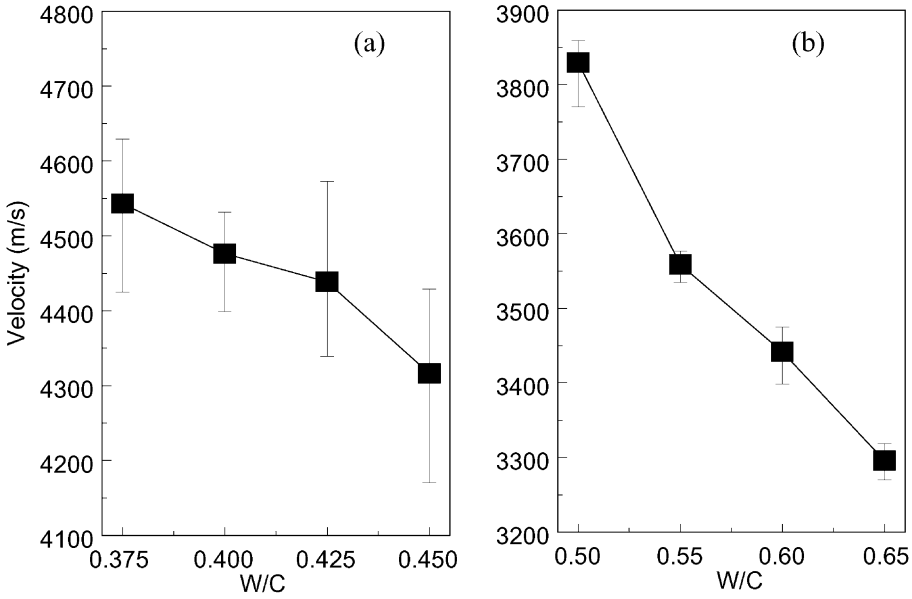

Fig. 10. Longitudinal wave velocity of (a) 2 days concrete and (b) of 1 day mortar.

not clearly observed in frequency domain, possibly due to the resonant behavior of the sensors.

The ratio of positive to negative area of the waveforms product, henceforth denoted as R_{pn}, was used as a classification rule of concrete specimens according to their water content. The multiplication of an individual waveform from a specimen of unknown composition with waveforms typical of each class and comparison of the R_{pn} ratios was proved a useful tool in classification of concrete AU signals.

The typical waveform for each class is calculated as the average of the waveforms originating from the same w/c ratio. So it contains information from 12 to 16 individual waveforms. For example, the typical waveform (signature) of the 0.375 class is the mathematical average of the 13 waveforms acquired from specimens with w/c = 0.375, while the typical waveform of the class 0.40 is the average of the 12 waveforms originating from specimens with w/c = 0.40, etc.

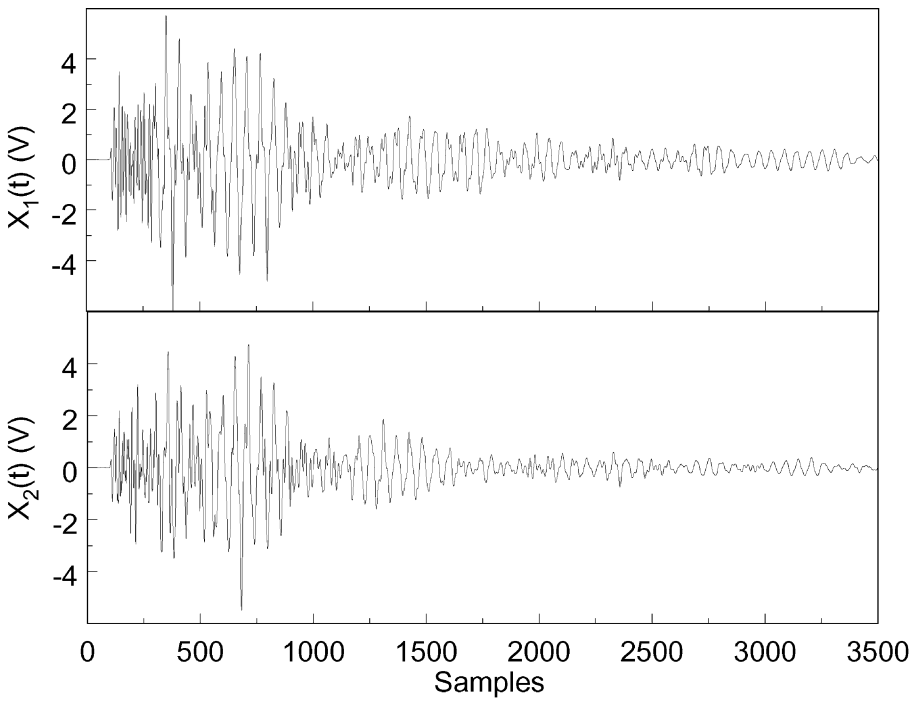

Fig. 11. Waveforms from two different specimens of w/c = 0.375 concrete at the age of 2 days.

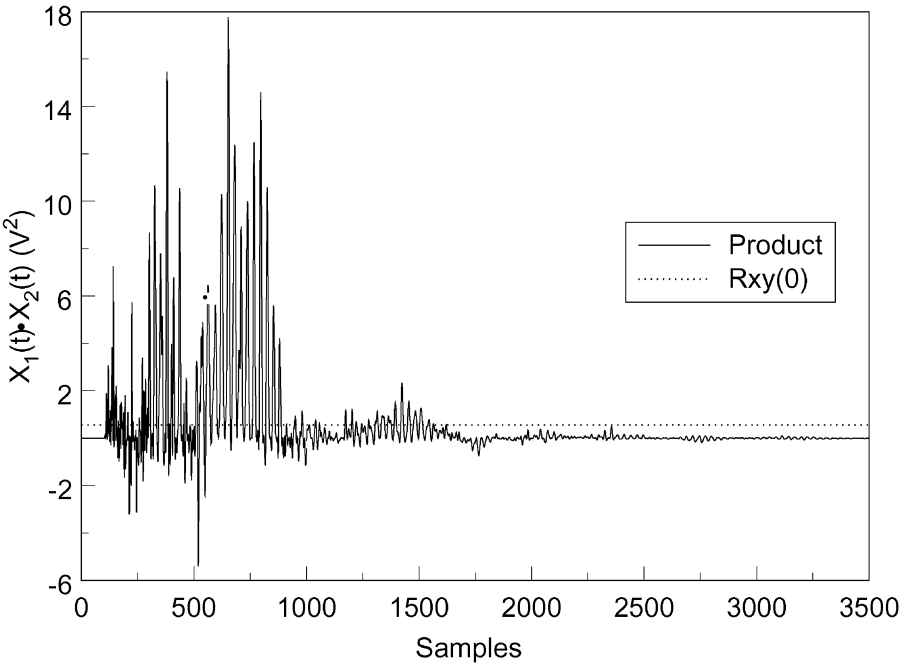

Fig. 12. Multiplication product of the waveforms of Fig. 11.

For a given age, e.g., 2 days, when a specific "unknown" waveform is presented, it is multiplied with all the typical waveforms concerning this age, i.e., the signatures of classes 0.375, 0.40, 0.425 and 0.45, and the values of R_{pn} are calculated. R_{pn} usually obtains values higher than 10, even 100, for waveforms of the same composition. On the contrary, for waveforms of different w/c ratio, it occasionally falls below unity. The waveform is classified to the class, with the signature of whom it exhibits the highest R_{pn} value. If this class is of the same w/c ratio with the specimen that the waveform originates from, this is considered a successful classification. This procedure is followed for the classifica-

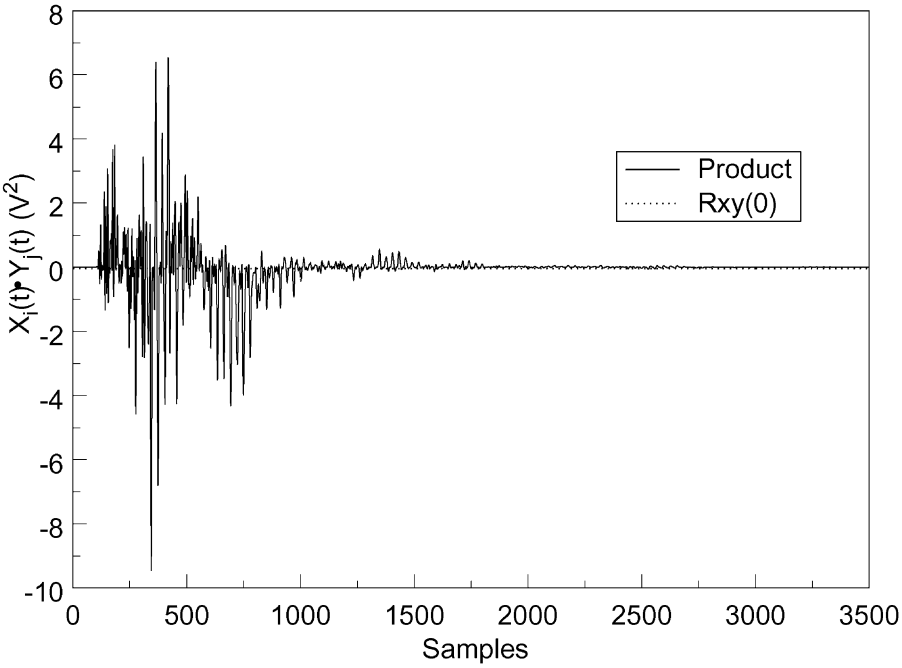

Fig. 13. Multiplication product of waveforms of w/c = 0.45 and w/c = 0.40 at the age of 2 days.

Table 1
Percentage (%) of successful classification per methodology according to age of concrete

Age	R_{pn}	ρ_{xy}	γ_{xy}^2
2	92.5	94.3	98.1
4	94.3	94.3	96.2
7	96.2	96.2	94.3
14	90.6	94.3	92.4
28	84.9	86.7	96.2
60	90.6	94.3	96.2
90	92.5	92.5	100

tion of all specimens of a certain age. The percentage of success for this age is defined as the ratio of successfully classified specimens to the total number of 53. After applying the R_{pn} scheme to all ages that AU measurements have been conducted, it was concluded that the success of this classification procedure is constantly held above 90%, with an average classification success of 92%, except for the age of 28 days (see Table 1). The best results are obtained at the age of 7 days, with the success percentage being as high as 96.2% (51 correct classifications out of 53 waveforms), while for the first week the success is almost 95%.

It should be mentioned that from the total 15,360 points of each waveform, only the first 3500 are considered important (1.75 ms) as in later times the signal is severely attenuated (see Figs. 4 and 5) and it is useless at all data points to be considered for the analysis. However, for some indicative cases, R_{pn} values were calculated also using the total number of points. The resulting R_{pn} values were not affected even on the third decimal digit.

3.3.2. Classification through the correlation coefficient

The efficiency of the R_{pn} scheme is attributed as stated above to the so-called synchronization of waveforms originating from similar material. It is known, however, that such similarities between two time functions, $X(t)$ and $Y(t)$, generally result in high correlation coefficients between the functions at hand. The correlation coefficient ρ_{xy}, being defined as:

$$\rho_{xy} = \frac{\sigma_{xy}}{\sigma_x \sigma_y} \qquad -1 \le \rho_{xy} \le 1 \tag{1}$$

where σ_{xy} stands for the covariance of $X(t)$ and $Y(t)$ and σ_x, σ_y the standard deviation of $X(t)$ and $Y(t)$, respectively, can also be used to quantify the synchronization between different waveforms. As seen in Fig. 14, stronger correlation is exhibited between points of waveforms of the same origin (ρ_{xy}=.793 in this case), while no essential relationship is observed concerning the points of different w/c waveforms (ρ_{xy}=.048).

Therefore, calculating the ρ_{xy} of any random waveform with the signatures of each class, the waveform is classified to the category with the signature of whom it exhibits the higher ρ_{xy}. The procedure is therefore simple, similar to the one described above, and leads to slightly improved percentages (see Table 1).

3.3.3. Use of coherence function

The classification approaches described so far are based on time domain characteristics of the signal. In order to take advantage of characteristics based on domains other than

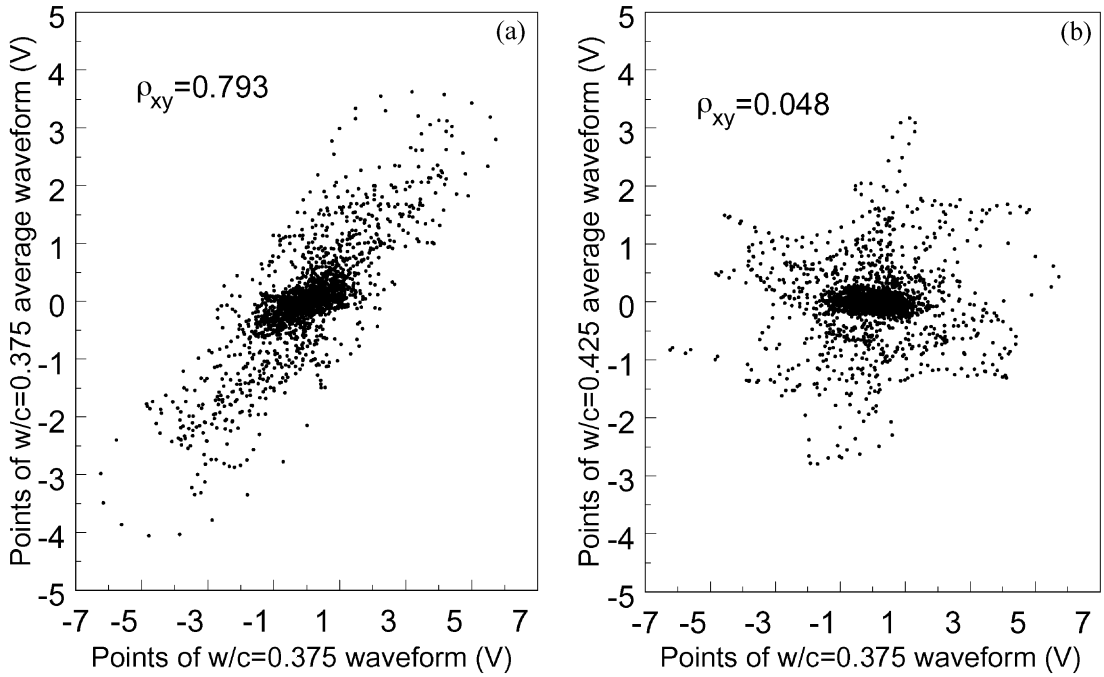

Fig. 14. Correlation plots between points of a 2-day specimen waveform of w/c = 0.375 and (a) the average waveform of w/c = 0.375 and (b) the average waveform of w/c = 0.425.

time, frequency characteristics should be examined. A similar approach was followed in Ref. [30], where the coherence function was used to quantify the similarity of AE signals emitted by identical fracture mechanisms in pull-out tests of concrete cubes. Coherence function is analogous to the squared correlation coefficient of time domain series underlying the frequency similarities of the signals and is given by Ref. [31]:

$$\gamma_{xy}^2(f) = \frac{|G_{xy}(f)|^2}{G_{xx}(f)G_{yy}(f)} \qquad 0 \le \gamma_{xy}^2(f) \le 1 \tag{2}$$

$G_{xy}(f)$ is the cross-spectral density function between $X(t)$ and $Y(t)$ and $G_{xx}(f)$, $G_{yy}(f)$ are the autospectral density functions of $X(t)$ and $Y(t)$, respectively, and is considered generally to be a more powerful tool than the correlation coefficient function in many applications [31].

It was observed that the mean value of the coherence function acquires higher values when $X(t)$ and $Y(t)$ belong to specimens of the same composition, as typically shown in Fig. 15 where the coherence functions between a w/c = 0.375 waveform and the signatures of classes 0.375 and 0.40 are depicted. The coherence function between the 0.375 waveform and the typical of its own class (γ_1^2) obtains higher values throughout almost all frequency bands than the typical of 0.40 (γ_2^2), resulting in a higher mean coherence (0.407 and 0.274, respectively).

Therefore, the mean value of the coherence function, calculated using MATLAB standard routines in this work, can be used also as a powerful classification rule, classifying a waveform to the class with the signature of whom it exhibits the highest mean coherence. Further, the mean coherence value was proved the most powerful tool examined in this work as to w/c ratio determination of hardened concrete as can be seen in Table 1, with success up to 100% (for 90 days concrete), while the success percentage for specimens up to 7 days lies above 96%.

Manufacturing fluctuations between different experimental phases, held in years 2000 and 2001, resulted in somewhat different 28-day compressive strengths (up to 6 MPa, about 12%) for the same compositions and even greater discrepancies in values of AU characteristics. Although this makes classical AU approach even harder than described in preceding paragraphs to be effective in classification, the tools described above proved insensitive to these fluctuations.

Thus, assuming that other important parameters of concrete mix design are held constant, e.g., the aggregate-to-cement ratio, type and grading of aggregates, the w/c ratio can be reliably estimated despite other manufacturing fluctuations.

It is clear that the use of the above methodologies is promising, although the population of specimens considered is quite low for establishment of engineering procedures for w/c ratio determination. However, these are the most efficient ways to characterize water content of concrete specimens involved in this experimental series. What is emphasized here is the procedure through which testing a small, albeit adequate, number of specimens with known composition will serve as a guide for concrete water content characterization. It is believed that the proposed methodologies could be a useful tool in concrete quality estimation, assuming the database population increases both in number of specimens and all applicable w/c categories.

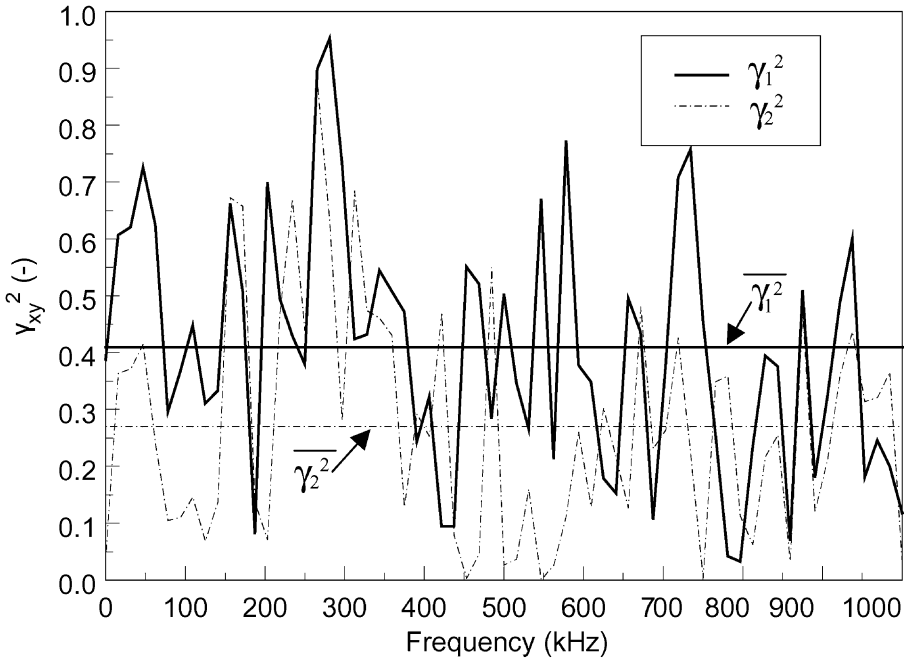

Fig. 15. Coherence functions γ_1^2(f), γ_2^2(f) between a waveform of w/c = 0.375 and the signatures of 0.375 and 0.40 classes.

4. Fresh paste

4.1. Experimental procedure

The AU setup for testing of fresh cement paste is in essence the same as the one described for the testing of hardened concrete, i.e., the same input pulse and piezoelectric sensors are used. The sampling rate though was set equal to 10 MHz since, in a preliminary investigation phase, broadband sensors were used which, however, for the specific propagation path and the heavily attenuative paste were not proven to be sensitive enough. In addition, a polyamide transparent jig with a cylindrical cavity is employed to constrain the liquid paste during the test (see Fig. 16). The cavity is filled with cement paste and the sensors are placed at the two ends being in direct contact with the paste. A simple pressuring device and two rubber o-rings ensure no liquid loss, while minimizing energy leak through the mass of the polyamide device. This is confirmed as when empty of paste, the arrival time of signals recorded from the cylindrical pot corresponds to the speed of sound in air.

The mixes consist of high-strength Portland cement and water, with five different w/c ratios from 0.45 to 0.65 with 0.05 w/c step between successive classes. The ingredients of

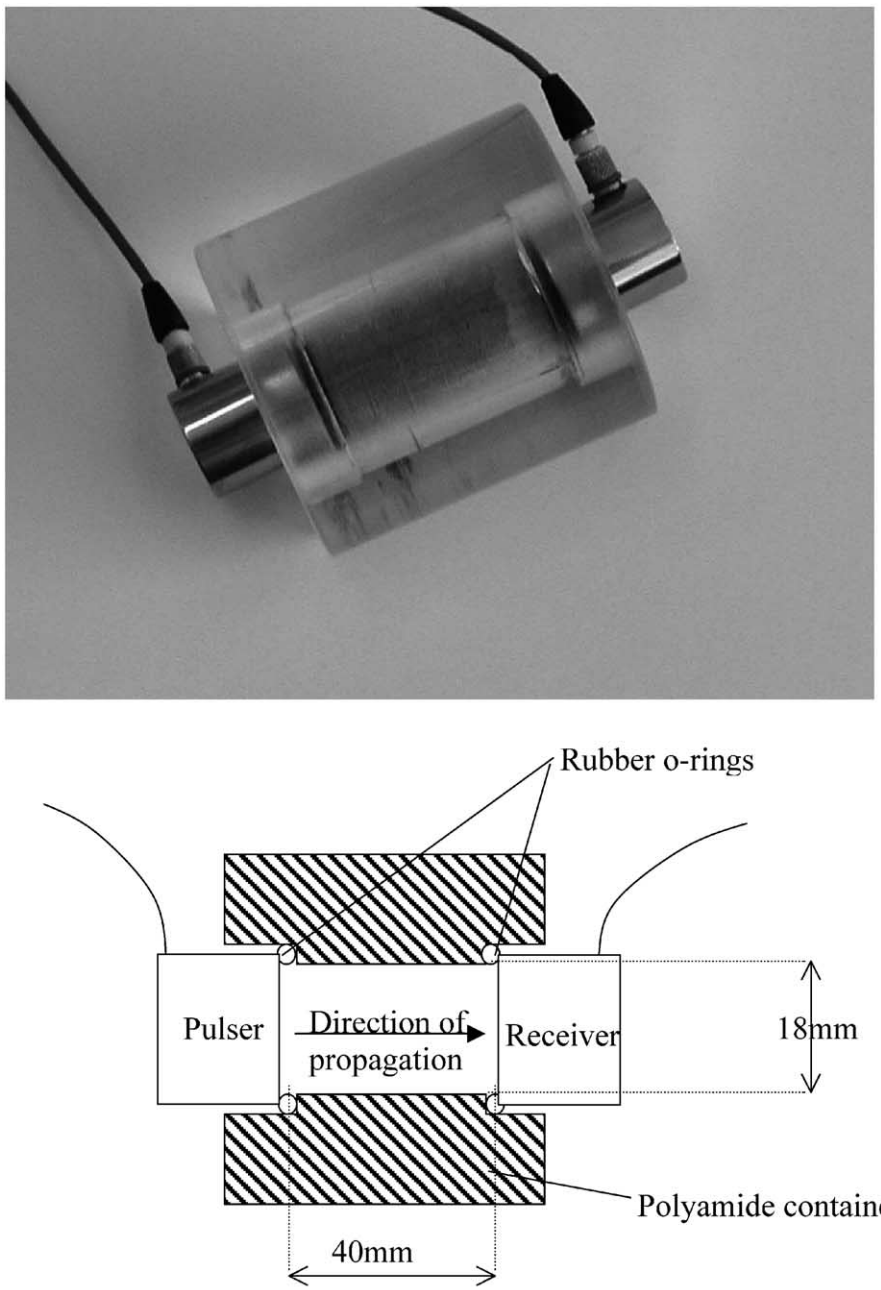

Fig. 16. Polyamide jig for fresh mortar testing.

any specimen are weighted separately with an accuracy of 0.1 mg, mixed and stirred for approximately 45 s. After the formed paste is poured into the polyamide pot, it is shaken for a period of about 1 min, resulting in the appearance of air bubbles on the upper part of the transparent pot and the initiation of the test is immediate. Each w/c class is formed of 10 specimens, while the results presented herein are based on waveforms obtained 3.5 min after the mixing of the ingredients.

4.2. Results and discussion

The wave propagation parameters measured are the same as in the case of hardened concrete, although different tendencies are revealed. Typical waveforms of specimens with different w/c ratios are presented in Fig. 17. A change in energy is generally observed for different water content as seen in Fig. 18 where also a slight increase in longitudinal wave velocity is observed for higher w/c ratios.

This seems contradictive to the results of hardened concrete. However, wave propagation in hardened concrete takes place primarily through the solid products formed after the hydration reaction between cement powder and water. On the other hand, in fresh paste of 3.5 min, gel has not yet been formed in sufficient quantities to allow wave propagation through itself. Thus, elastic waves propagate through the water present in the suspension and it seems that the higher the water content, the higher the wave energy transmitted through it. The experimental variance though is even higher than in hardened concrete AU tests, as revealed from the error bars shown in Fig. 18, corresponding to max and min values.

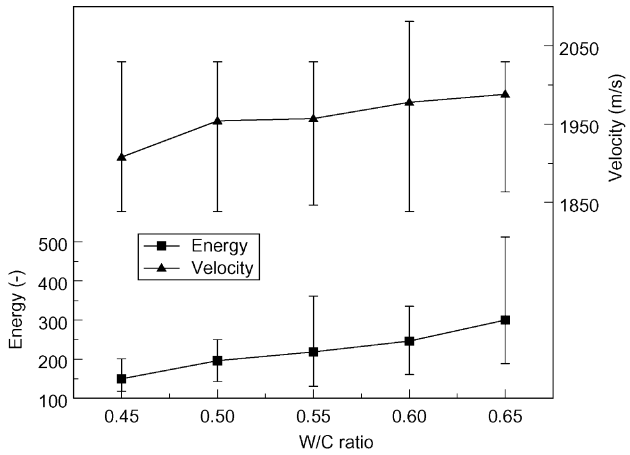

Fig. 18. Waveform energy and longitudinal wave velocity versus w/c ratio for fresh paste.

These findings, due to large scatter, seem even less promising than hardened concrete data, for a typical AU recognition approach to be undertaken. The schemes introduced earlier though, for w/c ratio determination of hardened concrete, and especially the mean value of the coherence function, provide easy and relatively reliable results for fresh paste as well resulting in 80% of correct classification.

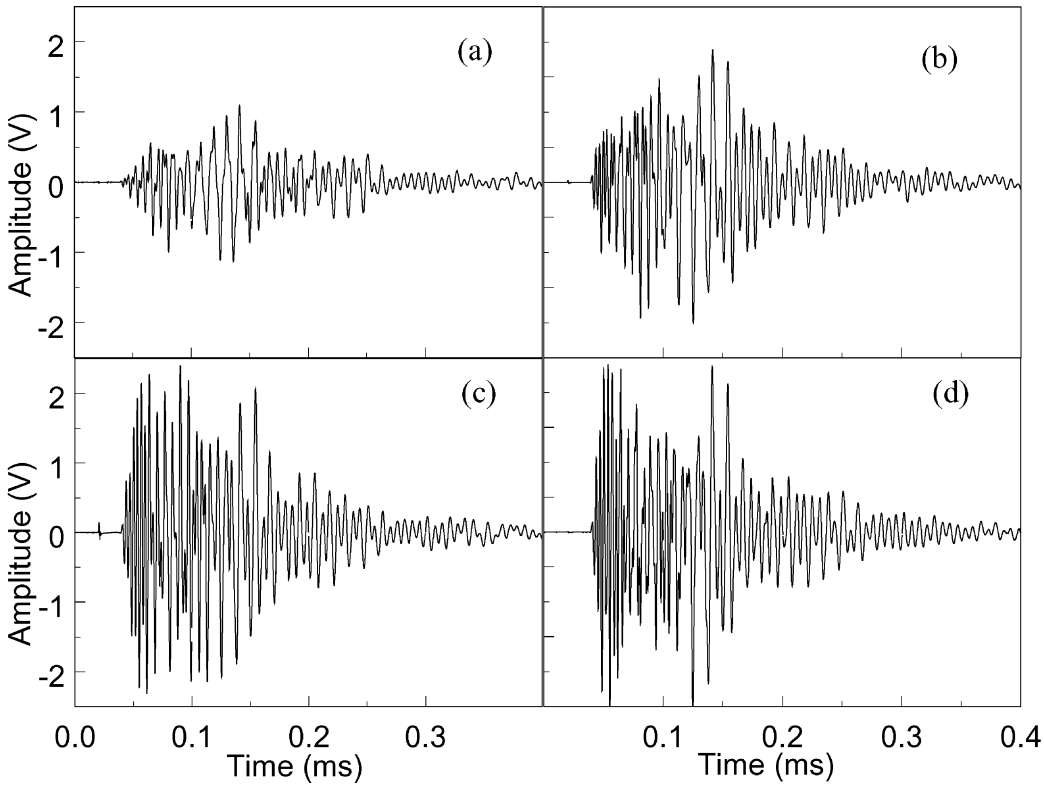

Fig. 17. Waveforms of fresh paste specimens with (a) w/c = 0.45, (b) w/c = 0.55, (c) w/c = 0.60, (d) w/c = 0.65.

Table 2
Percentage (%) of successful classification per methodology according to w/c of fresh paste

w/c	R_{pn}	ρ_{xy}	γ^2_{xy}
0.45	90	80	100
0.50	70	60	70
0.55	80	50	80
0.60	60	50	70
0.65	60	60	80
Total	72	60	80

4.3. Classification of fresh paste specimens

The classification approach remains the same as in hardened concrete. The characteristic waveforms (signatures) for the five different categories are calculated from the entire population of waveforms of each class. For any "unknown" waveform, the same procedures are applied like in the case of hardened concrete and the values of R_{pn}, ρ_{xy}, and γ^2_{xy} are determined.

The classification success of these procedures is quite encouraging, although not close to the success achieved for hardened concrete waveforms. The classification success for all w/c classes and methodologies is presented in Table 2. It is observed that the coherence function yields the highest percentage of correct classification, as is also the case for hardened concrete, being apparently more sensitive to wave propagation parameters typical of each w/c category. It can be seen that waveforms originated from the w/c = 0.45 category are more successfully classified, in contrast to the classes of w/c 0.60 and 0.65, where the success is below 80% independently of the characteristic used for classification. Nevertheless, the average percentage of success by the mean value of the coherence function is 80%, implying that increase of the experimental data should be sought in order to improve accuracy.

Indeed, the database is being currently enriched both in population, in order to yield statistically more reliable results, and in w/c classes to test the discriminative power of these descriptors, while efforts towards reducing variance of AU characteristics through modifications of the testing device are under consideration. Next step in this research project is the testing of fresh mortar and the establishment of a reliable testing and evaluation procedure for accurate determination of w/c ratio.

5. Conclusions

In the present work, results of AU measurements on hardened concrete and fresh paste are presented. The research concentrated on the w/c ratio influence on the propagating wave of materials with a/c ratio and type of aggregates being constant.

As was demonstrated, elastic wave propagation characteristics in concrete specimens are strongly correlated with the compressive strength and are influenced by age and water content. This was exploited by formulating a simple cross-correlation technique along with using the correlation coefficient and coherence function of different waveforms, as classification rules in determining w/c ratio of concrete. Considering the number of the specimens tested adequate, the proposed descriptors were proven valid criteria for the classification of specimens in the right w/c class. The success so far is high and it is believed that higher volume of experimental data, including more initial classes of w/c and more specimens for each class, will result in higher percentage of accuracy showing more clearly also which of the above classifiers is more powerful as to water content determination.

Extremely interesting and a field of current research engagement for the authors, is the application of such a technique on waveforms collected from fresh mortar and concrete, a few minutes after mixing, as the quality evaluation at such an early age is of even greater significance for in situ work, while preliminary results from tests of fresh paste seem promising.

Acknowledgements

The financial support of the Greek General Secretariat of Research and Technology in the framework of project ΕΠΕΤ#ΙΙ-83 (ΜΗΚΚΥΝΕΣ) is gratefully acknowledged.

The contribution of one of the reviewers in substantially improving the content and presentation of the original manuscript, especially by suggesting the use of the coherence function as a potential classifier, is also acknowledged.

References

[1] A.M. Neville, Properties of Concrete, Longman, London, 1995.
[2] M.F. Kaplan, The effects of age and water/cement ratio upon the relation between ultrasonic pulse velocity and compressive strength, Mag. Concr. Res. 11 (32) (1959) 85–92.
[3] D.A. Anderson, R.K. Seals, Pulse velocity as a predictor of 28- and 90-day strength, ACI J. 78–79 (1981) 116–122.
[4] L. Vergara, R. Miralles, J. Gosalbez, F.J. Juanes, L.G. Ullate, J.J. Anaya, M.G. Hernandez, M.A.G. Izquierdo, NDE ultrasonic methods to characterise the porosity of mortar, NDT E Int. 34 (2001) 557–562.
[5] T. Gudra, B. Stawinski, Non-destructive characterization of concrete using surface waves, NDT E Int. 33 (2000) 1–6.
[6] S. Popovics, J.S. Popovics, Ultrasonic testing to determine water–cement ratio for freshly mixed concrete, Cem., Concr. Aggreg. 20 (2) (1998) 262–268.
[7] A.T. Herb, H.W. Reinhardt, C.U. Grosse, Ultrasonic testing device for mortar, Otto-Graf-J. 10 (1999) 144–155.
[8] A. Boumiz, C. Vernet, F. Cohen Tenoudji, Mechanical properties of cement pastes and mortars at early ages, Adv. Cem. Based Mater. 3 (1996) 94–106.
[9] R. D'Angelo, T.J. Plona, L.M. Schwartz, P. Coveney, Ultrasonic measurements on hydrating cement slurries, Adv. Cem. Based Mater. 2 (1995) 8–14.
[10] C. Boutin, L. Arnaud, Mechanical characterization of heterogene-

ous materials during setting, Eur. J. Mech. A, Solids 14 (4) (1995) 633–656.
[11] S.K. Niyogi, P.K. Das Roy, M. Roychaudhuri, Acousto-ultrasonic study on hydration of portland cement, Ceram. Trans. 16 (1991) 137–145.
[12] T. Chotard, N. Gimet-Breart, A. Smith, D. Fargeot, J.P. Bonnet, C. Gault, Application of ultrasonic testing to describe the hydration of calcium aluminate cement at the early age, Cem. Concr. Res. 31 (2001) 405–412.
[13] S. Labouret, I. Looten-Baquet, C. Bruneel, J. Frohly, Ultrasound method for monitoring rheology properties evolution of cement, Ultrasonics 36 (1998) 205–208.
[14] M.I. Valic, Hydration of cementitious materials by pulse echo USWR Method, apparatus and application examples, Cem. Concr. Res. 30 (2000) 1633–1640.
[15] T. Ozturk, J. Rapoport, J.S. Popovics, S.P. Shah, Monitoring the setting and hardening of cement-based materials with ultrasound, Concr. Sci. Eng. 1 (1999) 83–91.
[16] J. Keating, D.J. Hannant, A.P. Hibbert, Correlation between cube strength, ultrasonic pulse velocity and volume change for oil well cement slurries, Cem. Concr. Res. 19 (5) (1989) 715–726.
[17] J.R. Rapoport, J.S. Popovics, S.V. Kolluru, S.P. Shah, Using ultrasound to monitor stiffening process of concrete with admixtures, ACI Mater. J. 97 (6) (2000) 675–683.
[18] V. Garnier, G. Corneloup, J.M. Sprauel, J.C. Perfumo, Setting time study of roller compacted concrete by spectral analysis of transmitted ultrasonic signals, NDT E Int. 28 (1) (1995) 15–22.
[19] C.U. Grosse, H.W. Reinhardt, Fresh concrete monitored by ultrasound methods, Otto-Graf-J. 12 (2001) 157–168.
[20] V.M. Malhotra, N.J. Carino (Eds.), CRC Handbook on Nondestructive Testing of Concrete, CRC Press, Florida, 1991.
[21] T. Uomoto (Ed.), Non-Destructive Testing in Civil Engineering, Elsevier, Amsterdam, 2000.
[22] A. Vary, The acousto-ultrasonic approach, in: J.C. Duke (Ed.), Acousto-Ultrasonics: Theory and Application, Plenum, New York, 1988.
[23] A. Fahr, Y. Youssef, S. Tanary, Adhesive bond evaluation using acousto-ultrasonics and pattern recognition analysis, J. Acoust. Emiss. 12 (1–2) (1994) 39–44.
[24] E.H. Kautz, Determination of plate wave velocities and diffuse field decay rates with broadband acousto-ultrasonic signals, J. Acoust. Emiss. 12 (1–2) (1994) 65–70.
[25] H.L.M. dos Reis, Acousto-ultrasonic nondestructive evaluation of porosity in polymer-composite structures of complex geometry, J. Acoust. Emiss. 12 (1–2) (1994) 15–21.
[26] A.F. Beall, M.J. Biernacki, L.R. Lemaster, The use of acousto-ultrasonics to detect biodeterioration in utility poles, J. Acoust. Emiss. 12 (1–2) (1994) 55–64.
[27] D.E. Bray, D. McBride (Eds.), Nondestructive Testing Techniques, Wiley, New York, 1992.
[28] D.G. Aggelis, D. Polyzos, T.P. Philippidis, A. Tsimogiannis, A. Anastasopoulos, B. Georgali, B. Kaloidas, Non destructive estimation of mortar's composition and strength using acousto-ultrasonics, Proceedings of the First Hellenic Conference on Concrete Composite Materials, Xanthi, 2000, pp. 49–71 (in Greek).
[29] D.G. Aggelis, T.P. Philippidis, K.K. Sideris, Mortar's compressive strength estimation using the method of acousto-ultrasonics, Proceedings of the First Hellenic Conference on Concrete Composite Materials, Xanthi, 2000, pp. 72–85 (in Greek).
[30] C. Grosse, H. Reinhardt, T. Dahm, Localization and classification of fracture types in concrete with quantitative acoustic emission measurement techniques, NDT E Int. 30 (4) (1997) 223–230.
[31] J.S. Bendat, A.G. Piersol, Engineering Applications of Correlation and Spectral Analysis, 2nd ed., Wiley, New York, 1993.